J Mater Sci: Mater Med (2009) 20:105–111
DOI 10.1007/s10856-008-3545-8

Fabrication of porous poly(L-lactide) (PLLA) scaffolds for tissue engineering using liquid–liquid phase separation and freeze extraction

L. Budyanto · Y. Q. Goh · C. P. Ooi

Received: 30 April 2008 / Accepted: 15 July 2008 / Published online: 14 August 2008

Abstract PLLA scaffolds were successfully fabricated using liquid–liquid phase separation with freeze extraction techniques. The effects of different processing conditions, such as method of cooling (direct quenching and pre-quenching), freezing temperature (−80°C and −196°C) and polymer concentration (3, 5 and 7 wt%) were investigated in relations to the scaffold morphology. SEM micrographs of scaffolds showed interconnected porous network with pore size ranging from 20 to 60 μm. The scaffolds had porosity values ranging from 80 to 90%. Changes to the interconnected network, porosity and pore size were observed when the method of cooling and polymer concentration was changed. Direct quenching to −80°C gave a more porous interconnected microstructure with uniform pore size compared to samples prepared using pre-quenching method. Larger pores were observed for samples quenched at −80°C compared to −196°C. Scaffolds prepared using direct quenching to −196°C had higher elastic modulus and compressive stress compared to those quenched to −80°C. The compressive elastic modulus ranged from 4 to 7 MPa and compressive stress at 10% strain was from 0.13 to 0.18 MPa.

1 Introduction

Tissue engineering is a new emerging field which serves as an alternative solution to repair defective tissues and organ, instead of relying on conventional organ transplantation. There are several requirements to be met by biodegradable scaffolds employed in tissue engineering application, such as high porosity, adequate pore size, interconnected pore network, biocompatibility and biodegradability [1–3]. Mechanical property of the scaffolds is another important parameter, where the scaffolds should be able to maintain the integrity of the designed structure and provide sufficient temporary mechanical support to withstand stresses and loading associated with their applications [4].

Synthetic biodegradable polymer, poly(α-hydroxyl acids) is one of the most important class and frequently used polymer in tissue engineering. Poly(glycolic acid) (PGA), poly(lactic acid) (PLA) and poly(lactic-co-glycolic acid) (PLGA) have received approval from US Food and Drug Administration (FDA) for human clinical use [2, 5]. Numerous techniques have been reported in the literature for the fabrication of biodegradable scaffolds, such as gas foaming, fiber bonding, solvent casting/particulate leaching, thermally induced phase separation (TIPS), and 3D-printing [6–9].

Here, a thermally induced phase separation (TIPS) process was used to fabricate porous biodegradable tissue engineering scaffolds. This technique uses thermal energy as a driving force to induce phase separation [9]. TIPS can be divided into solid–liquid and liquid–liquid phase separation. The main difference between these two processes is the miscibility of the system. Strong polymer-solvent interaction leads to solid-liquid phase separation, whereas weak polymer-solvent interaction will result in liquid–liquid phase separation [10]. Addition of non-solvent is usually carried out to lower the degree of polymer-solvent interaction, as a means to induce liquid–liquid phase separation [11]. By varying the phase separation conditions, such as types of polymer and solvent, polymer concentration, solvent/non-solvent ratio, and thermal quenching strategy, different porous structures can be obtained [12–14].

L. Budyanto · Y. Q. Goh · C. P. Ooi (✉)
Division of Bioengineering, School of Chemical and Biomedical Engineering, Nanyang Technological University, Singapore 639798, Singapore
e-mail: ASCPOoi@ntu.edu.sg

In the case of TIPS, freeze drying is usually required for solvent removal to retain the porous structure of the scaffolds [11, 15–17]. This method has several disadvantages. Besides being time and energy consuming, it has a problem of surface skin formation. Ho et al. [18] solved these problems using freeze extraction, which immerses frozen polymer solution into non-solvent bath. This facilitates the exchange of solvent and non-solvent, resulting in similar porous structure without the surface skin. Recently, highly porous PLLA scaffolds were successfully created using solid-liquid phase separation technique, together with freeze extraction. The scaffolds had anisotropic tubular morphology with an internal ladder-like structure [19].

In this paper, porous PLLA scaffolds were fabricated using liquid–liquid phase separation technique together with freeze extraction, instead of the commonly used freeze drying. The changes in scaffold morphology were investigated by varying the processing parameters, such as cooling methods, freezing temperature, and polymer concentration. The corresponding mechanical properties of the scaffolds were also reported.

2 Experimental

2.1 Materials

Poly(L-lactide), PLLA with inherent viscosity of 1.04 dl/g, M_w of 95,000 g/mol was purchased from Fluka. 1,4-dioxane of ReagentPlus® Grade, ≥99% purity, was purchased from Sigma Aldrich Pte Ltd. Ethanol of analytical grade was purchased from Sino Chemical Company Pte Ltd.

2.2 Measurement of cloud point

The cloud point temperatures for the PLLA/1,4-dioxane/water ternary system were determined by means of visual turbidimetry. PLLA (1, 3, 5 7 and 10 wt%) was dissolved in 1,4-dioxane/water mixture (87/13, wt/wt) in a 100 cm^3 flask, by heating and stirring the solution at 60°C for 2 h. After dissolution, the temperature of the solution was increased to 80°C. The clear solution was then slowly cooled at a rate of 1°C/min and the cloud point temperature was recorded. Cloud point temperature was defined as the temperature at which the solution turned cloudy, as observed visually.

2.3 Fabrication of PLLA scaffolds

PLLA (3, 5 and 7 wt%) was dissolved in a mixture of 1,4-dioxane and water (87/13, wt/wt) by heating the solution to 60°C for 2 h. The solution was then heated to 15°C above the cloud point temperature. In the study of different freezing temperatures, the samples were immediately quenched to –80°C (freezer) and −196°C (liquid nitrogen). In the study of cooling methods, the samples were pre-quenched to 25°C for 5 min in a 25°C water bath, before they were transferred into a freezer at −80°C or liquid nitrogen at −196°C. The mixture of 1,4-dioxane and water was then removed using freeze extraction. The frozen polymer sample was immersed into 150 ml of 80 wt% ethanol aqueous solution that was pre-cooled to −24°C for 2 days. The samples were then dried at room temperature for another 2 days to remove the aqueous ethanol solution. The samples were kept in a dessicator cabinet at 22°C and 40% relative humidity prior to characterization.

2.4 Characterization of PLLA scaffolds

The morphology of the scaffolds was investigated using scanning electron microscopy (SEM JOEL JSM 6390LA). Longitudinal sections of the samples were coated with platinum for 80 s at 10 mA prior to SEM analysis. The pore size was estimated from an average of 10 readings for each sample.

The thermal properties of the PLLA scaffolds, including melting points (T_m) and corresponding enthalpy changes (ΔH_m), were measured by a Mettler Toledo DSC822e Differential Scanning Calorimeter. 2.5 mg of sample was used for each run. The measurement was carried out at a heating rate of 5°C/min and with a scanning range of 25–220°C. The degree of crystallinity, X_c, was computed as [20]:

$$X_c = \frac{\Delta H_m}{\Delta H_m^o} \quad (1)$$

where ΔH_m^o is the enthalpy of melting for 100% crystalline PLLA (203.4 Jg^{-1}) [20].

The porosity, ε, of PLLA scaffolds was determined using Eq. 2 [19]:

$$\text{Total Porosity, } \varepsilon = \frac{D_p - D_f}{D_p} \times 100\ \% \quad (2)$$

where D_f is the scaffold density and D_p is the polymer skeletal density, which is defined as

$$D_p = \frac{1}{\frac{1-X_c}{D_a} + \frac{X_c}{D_c}} \quad (3)$$

where the density for completely amorphous PLLA, D_a, is 1.248 gml^{-1} and the density for completely crystalline PLLA, D_c, is 1.290 gml^{-1} [21].

Quantification of scaffolds' compressive properties is important as it is one of the predominant loading modes they will experience in vivo [22]. The compressive mechanical properties of the scaffolds were tested using an INSTRON universal testing machine (model 5569) with Bluehill software. Samples were cut into prism of uniform

sizes ($1.3 \times 1.3 \times 2.5$ cm^3), according to the guidelines set in the ASTM D695-02a. A 50 kN load cell and crosshead speed of 1 mm/min were used in this study. Elastic modulus of the scaffold was determined from the initial linear region of the compressive stress–strain curve, while the plastic modulus was determined by the slope of the curve in the plastic region. Compressive stress at 10% strain (σ_{10}) and the end point of linear plateau region (S_{end}) which indicated the beginning of scaffold densification were also measured. Results were reported as an average of five measurements.

3 Results and discussions

3.1 Measurement of cloud point temperature

Cloud point determination can be utilized as a good criterion dividing the homogeneous and phase separated region [9], where the critical phase separation temperature (T_c) and the critical polymer concentration (φ_c) can be obtained from a cloud point curve. The cloud point temperatures for different concentrations of PLLA in 1,4-dioxane and water mixture are presented in Fig 1. The turbidity transition for this ternary system was sharp, as a result of liquid–liquid de-mixing instead of crystallization process [23]. The cloud point temperatures increased gradually with increasing polymer concentration as observed in Fig. 1.

3.2 Effect of freezing temperature on scaffold morphology

5 wt% PLLA solution was directly quenched from 15°C above the cloud point temperature to two different freezing temperatures (−80°C and −196°C). Figure 2 shows the resulting scaffold morphologies at the two different freezing temperatures. The scaffolds had isotropic porous network with average pore size ranging from 20 to 60 μm. Direct quenching to −80°C resulted in larger pores (47 ± 8) with better interconnectivity compared to −196°C (22 ± 4). This observation is in agreement with literature [24], where lower freezing temperature resulted in scaffolds with smaller pore structures and vice versa. Pore formation in scaffolds fabricated by liquid–liquid phase separation is caused by the solvent crystallization process in the polymer solution. Solvent crystallization process is highly dependent on the solution cooling rate [15], which is in turn, determined by the freezing temperature of the polymer solution. In other words, the lower freezing temperature (−196°C) had a larger temperature gradient to equilibrium, which resulted in faster cooling rate and less time for solvent nucleation, crystal growth and phase separation to occur. Hence the smaller pores in the scaffolds. Tu et al. also reported that higher freezing temperature is favoured to obtain large crystals of dioxane solvent, leading to large pores in the scaffolds [17]. Table 1 shows the pore size and porosity of 5 wt% PLLA scaffolds fabricated at two different freezing temperatures.

From Table 1, the change in freezing temperature had little influence on the porosity of 5 wt% PLLA scaffolds. All scaffolds had high porosity (>80%), which is suitable for tissue engineering applications.

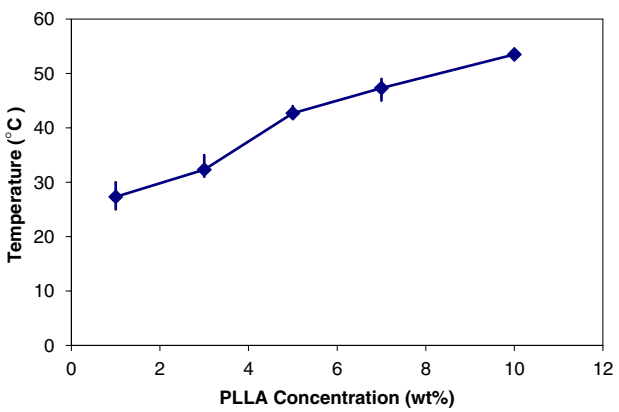

Fig. 1 Cloud point temperature at different PLLA concentrations

3.3 Effect of pre-quenching on scaffold morphology

The 5 wt% PLLA solution was pre-quenched from 15°C above cloud point temperature to 25°C for 5 min, followed by freezing at −80°C in the freezer or at −196°C in liquid nitrogen. The resulting pore morphologies are observed in Fig. 3. The scaffolds appeared to be less interconnected compared to scaffolds fabricated from direct quenching (Fig. 2). These scaffolds also showed a porous network with a combination of large (up to 50 μm) and small (10–25 μm) pores. Hence the pre-quenching step at 25°C increased the size distribution and decreased the interconnectivity of the pores.

It is believed that the final scaffold morphology relies on the thermodynamic state of the solution to be quenched [11]. If the polymer solution is quenched to a temperature between the binodal and spinodal curve, liquid–liquid phase separation occurs via nucleation and growth mechanism. On the other hand, polymer solutions quenched directly to temperatures below the spinodal curve will undergo spinodal decomposition [16]. A nucleation and growth mechanism type of phase separation results in a poorly connected stringy or beady structure, while spinodal phase separation is expected to give rise to a well interconnected structure with uniform pores [15].

The spinodal area could only be entered directly at a critical polymer concentration, ϕ_c. Previous studies have shown that the critical concentration (ϕ_c) for PLLA

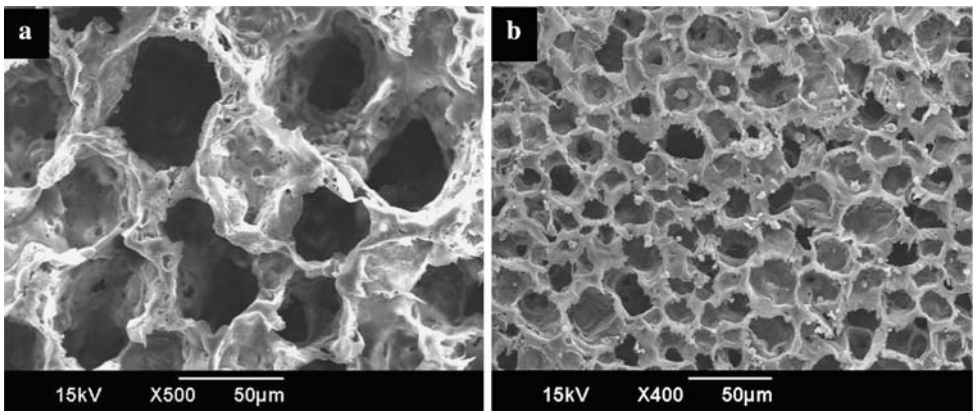

Fig. 2 SEM longitudinal section of 5 wt% PLLA scaffolds by liquid–liquid phase separation and freeze extraction technique, direct quenching to (**a**) −80°C and, (**b**) −196°C

Table 1 Pore size and porosity of 5 wt% PLLA scaffolds fabricated using direct quenching

Freezing temperature (°C)	Pore size (μm)	Porosity (%)
−80	47 ± 8	89.5
−196	22 ± 4	88.2

solution in 1,4-dioxane/water mixture (87/13, wt/wt) is around 4–4.5 wt% [15]. In all other concentrations, the metastable area between the binodal and spinodal curve must first be passed [23]. It is believed that the 5 wt% polymer solution entered the metastable area in the pre-quenching step at 25°C, where phase separation occurred via nucleation and growth mechanism. This gave rise to scaffolds with poorly interconnected pores of various sizes. In the direct quenching process to −80°C and −196°C, the high cooling rates prevented phase separation in the metastable area. A bicontinuous structure was obtained, where both the polymer-rich and polymer-lean phases were completely interconnected as a result of spinodal decomposition. Scaffold with a continuous pore network was thus obtained as observed in Fig 2. This observation affirms that the residence time in the binodal region before crossing the spinodal line is a crucial factor controlling the scaffold morphology as reported by Li et al. [25].

Table 2 Pore size and porosity of 5 wt% PLLA scaffolds pre-quenched at 25°C for 5 min followed by freezing at −80°C and −196°C

Freezing temperature (°C)		Pore size (μm)	Porosity (%)
−80	Small pores	18 ± 4	82.4
	Large pores	40 ± 11	
−196	Small pores	14 ± 5	81.3
	Large pores	32 ± 8	

Table 2 shows the pore size and porosity of 5 wt% PLLA scaffolds fabricated with the pre-quenching step. Scaffolds fabricated by pre-quenching at 25°C had slightly lower porosity as compared to those fabricated using direct quenching (~89% from Table 1). The small difference in the scaffolds' porosity suggests that the different cooling methods used here had limited influence on the final scaffolds' porosity. However, the average pore sizes of the scaffolds indicated that scaffolds fabricated by pre-quenching at 25°C had larger pore size distribution than those from direct quenching. This was observed from the obvious sets of small (10–25 μm) and large (up to 50 μm) pore sizes in Table 2.

Scaffolds fabricated by direct quenching to −80°C with uniformly distributed pores and interconnected network,

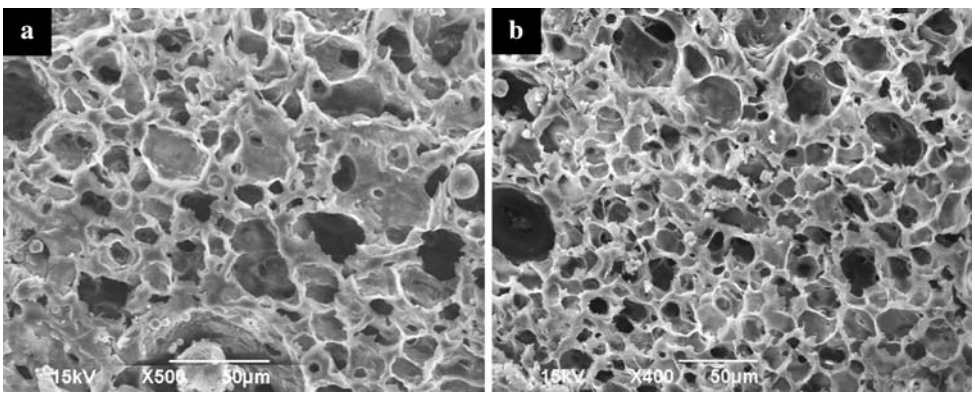

Fig. 3 SEM longitudinal section of 5 wt% PLLA scaffolds by liquid–liquid phase separation and freeze extraction technique pre-quenched at 25°C for 5 min followed by freezing at (**a**) −80°C and, (**b**) −196°C

such as those in Fig. 2, facilitate homogenous tissue formation throughout the scaffolds and are usually preferred for tissue engineering applications.

3.4 Effect of polymer concentration on scaffold morphology

Three different PLLA concentrations of 3, 5 and 7 wt%, were used to fabricate scaffolds by directly quenching the PLLA solution from 15°C above the cloud point temperature to −80°C. No scaffold was obtained from 3 wt% PLLA, where powder-like solid was observed after solvent removal by freeze extraction. Scaffold architecture was only observed for 5 and 7 wt% PLLA. Scaffolds from 5 wt% PLLA had interconnected porous structure with spherical pores of average pore diameter of (47 ± 8) μm (Table 1), while scaffolds from 7 wt% PLLA exhibited closed-pore structure with very poor interconnectivity (Fig. 4). The pore size and porosity of the 7 wt% scaffolds were found to be (38 ± 4) μm and 76.2% respectively.

At 3 wt% PLLA, the polymer concentration was below the critical polymer concentration, where the polymer-lean phase was the dominant phase in comparison to the polymer-rich phase. This led to the formation of polymer-rich droplets dispersed throughout the polymer-lean matrix, causing the scaffold structure to collapse and end up as powder upon solvent removal. As for 7 wt% PLLA, the polymer concentration was above the critical polymer concentration. In this case, droplets of polymer-lean phase were formed in a matrix of polymer-rich phase due to higher fraction of polymer-rich phase in comparison to polymer-lean phase. The result was PLLA scaffold with closed-pore structure as observed in Fig. 4.

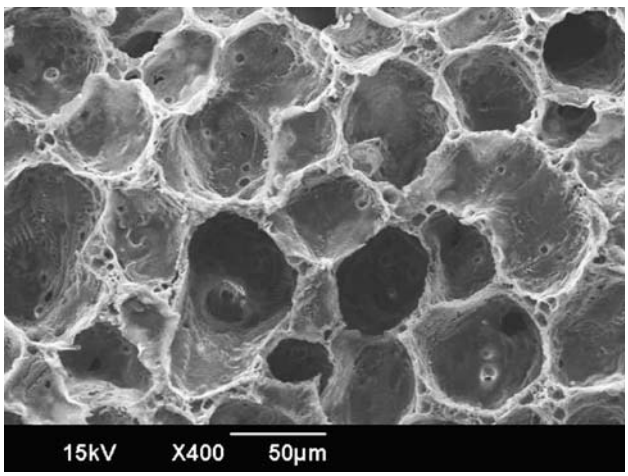

Fig. 4 SEM micrographs of 7 wt% PLLA scaffolds by liquid–liquid phase separation and freeze extraction technique, 400× magnification, direct quenching to −80°C

The scaffolds fabricated in this study using liquid–liquid phase separation with freeze extraction techniques were of similar morphology to the PLLA scaffolds fabricated by liquid–liquid phase separation with freeze drying techniques [9, 15]. All scaffolds exhibited isotropic porous network with fair to good interconnectivity depending on the polymer concentration and processing conditions employed.

3.5 Thermal properties of PLLA scaffolds

All of the samples showed a melting peak temperature, T_m of (176.7 ± 0.1)°C. This melting temperature was similar to the as-received PLLA (Table 3). The variation in processing parameters, such as cooling methods, freezing temperature and, polymer concentration did not affect the semicrystalline morphologies of the scaffolds, which were similar to the as-received polymer.

The degree of crystallinity, X_c, of the samples prepared from 5 wt% PLLA remained unchanged, within experimental error, with respect to different processing parameters. The X_c was (25 ± 3) % and was similar to that of as-received PLLA. However, samples prepared from 7 wt% solution exhibited slightly higher degree of crystallinity when compared to the 5 wt% samples. This might also account for the smaller pore structures in the 7 wt% PLLA scaffolds compared to the 5 wt% PLLA scaffolds fabricated under the same processing conditions. Hence polymer concentration influenced the degree of crystallinity and thus the pore size and porosity of the fabricated scaffolds, to a certain extent.

3.6 Mechanical properties

Scaffolds fabricated by direct quenching method were chosen for compressive mechanical testing because they exhibited preferred morphology for tissue engineering application compared to scaffolds fabricated using the pre-quenching step. These scaffolds showed highly porous and interconnected network, with narrow pore size distribution.

Figure 5 displays the stress–strain curve of 5 wt% PLLA scaffold prepared using direct quenching at −80°C. The profile is a classical compressive stress–strain curve of samples with porous structures. The curve was divided into linear elastic section, flat section, and densified section [22, 26]. The linear elastic section represented linear elastic deformation at small strain, whereas the flat section was the plateau region at larger strain. The last section of the curve (densified section) occurred when the scaffold was increasingly solidified, thus the stress increased sharply at very large strain. The rapid increase of the stress was most likely due to the collapse of the pore-walls of the scaffolds.

Table 3 Thermal properties of scaffolds fabricated with different cooling methods, freezing temperature, and polymer concentration

Concentration (wt%)	Freezing temperature (°C)	Pre-quenching step	Melting temperature (°C)	Degree of crystallinity (%)
As-received PLLA	–	–	176.79	25.2
5	−80	Yes	176.75	20.5
5	−80	No	176.58	26.3
5	−196	Yes	176.50	26.3
5	−196	No	176.75	27.3
7	−80	No	177.00	30.5

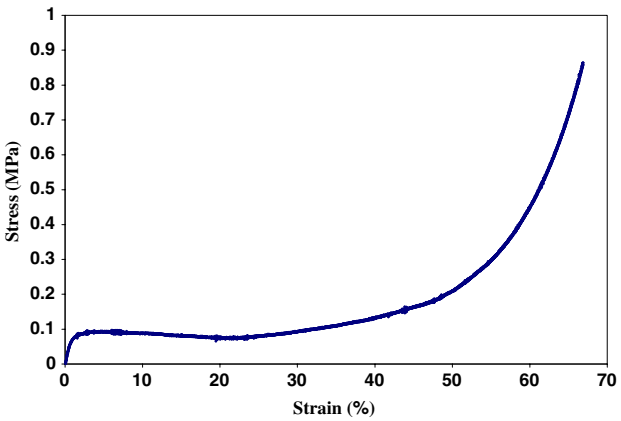

Fig. 5 Compressive stress–strain curve for 5 wt% PLLA scaffolds fabricated using liquid–liquid phase separation and freeze extraction technique, direct quenching to −80°C

The compressive mechanical properties of 5 wt% PLLA scaffolds prepared using direct quenching at −80°C and −196°C are summarized in Table 4. The results are reported as an average of five measurements.

The scaffolds fabricated by direct quenching to −196°C exhibited larger elastic and plastic modulus and compressive stress at 10% strain, in comparison to those quenched to −80°C. Both the scaffolds had similar porosity values (∼89%) and degree of crystallinity (∼27%). However, the average pore sizes of these two scaffolds were different. Scaffolds with direct quenching to −196°C had smaller pore size compared to those quenched to −80°C. Hence pore size might have affected the compressive mechanical properties to a larger extent than the porosity or crystallinity of the PLLA scaffolds.

As shown in Table 4, scaffolds fabricated in this study possessed sufficient mechanical properties for tissue engineering application, such as cartilage [27]. The compressive stiffness for the scaffolds ranged from 4 to 7 MPa and compressive stress at 10% strain (σ_{10}) was from 0.13 to 0.18 MPa.

4 Conclusions

PLLA scaffolds were successfully fabricated using liquid–liquid phase separation with freeze extraction techniques. Changes in processing parameters, such as cooling method freezing temperature and, polymer concentration affected the resultant scaffold morphology.

Scaffolds fabricated by direct quenching exhibited preferred morphology for tissue engineering applications compared to scaffolds fabricated using pre-quenching step. These scaffolds showed highly porous and interconnected network, with uniform pore size distribution. The concentration of polymer affected the pore size and porosity of the scaffolds. The average pore size and porosity of scaffold increased with decreasing polymer concentration. 5 wt% PLLA solution in 1,4-dioxane/water mixture (87/13, wt/wt) was the best composition for scaffold fabrication compared to 3 and 7 wt% PLLA. The porosity measured for these 5 wt% PLLA scaffolds was high, in the range of 81% to 89%. The pore interconnectivity was found to decrease with polymer concentration. As for compressive strength, the scaffolds produced by direct quenching to −80°C and −196°C exhibited adequate compressive mechanical properties necessary for tissue engineering applications. The compressive stiffness ranged from 4 to 7 MPa and compressive stress at 10% strain was from 0.13 to 0.18 MPa. Since high porosity and good interconnectivity are crucial for the success of tissue engineering applications, the preferred processing parameters for fabrication of PLLA scaffolds using liquid–liquid phase separation with

Table 4 Compressive mechanical properties of 5 wt% PLLA scaffolds fabricated using direct quenching

Sample	$E_{elastic}$ (MPa)	$E_{plastic}$ (MPa)	σ_{10} (MPa)	S_{end} (%)
Direct quenching to −80°C	4.4 ± 0.5	1.4 ± 0.3	0.13 ± 0.01	48 ± 3
Direct quenching to −196°C	7.5 ± 1.3	2.4 ± 0.2	0.18 ± 0.03	55 ± 2

freeze extraction techniques were PLLA of concentration above 5 wt%, with direct quenching to −80°C.

References

1. J.H. Lee et al., Biomaterials **24**(16), 2773–2778 (2003)
2. P.X. Ma, Materials Today **7**(5), 30–40 (2004)
3. Y. Cao et al., in *Biopolymer Methods in Tissue Engineering*, ed. by A.P. Hollander, P.V. Hatton (Humana Press, 2004), pp. 87–111
4. D.L. Butler, S.A. Goldstein, F. Guilak, J Biomech Eng **122**(6), 570–575 (2000)
5. R. Thomson et al., in *Biopolymers* II, ed by N.A. Peppas, R.S. Langer (Springer Berlin/Heidelberg, 1995), pp. 245–274
6. L.D. Harris, B.-S. Kim, D.J. Mooney, J Biomed Mater Res **42**(3), 396–402 (1998)
7. A.G. Mikos et al., J Biomed Mater Res **27**(2), 183–189 (1993)
8. H.-R. Lin et al., J Biomed Mater Res **63**(3), 271–279 (2002)
9. Y.S. Nam, T.G. Park, J Biomed Mater Res **47**(1), 8–17 (1999)
10. S.S. Kim, D.R. Lloyd, Polymer **33**(5), 1047–1057 (1992)
11. C. Schugens et al., Polymer **37**(6), 1027–1038 (1996)
12. S. Yang et al., Tissue Eng **7**(6), 679–689 (2001)
13. A.G. Mikos, J.S. Temenoff, Electron J Biotechnol **3**(2), 114–119 (2000)
14. R. Zhang, P. X. Ma in *Methods of tissue engineering*, ed. by A. Atala, R.P. Lanza (Academic Press, 2002), pp. 715–724
15. F.J. Hua, T.G. Park et al., Polymer **44**(6), 1911–1920 (2003)
16. F.J. Hua, G.E. Kim et al., J Biomed Mater Res **63**(2), 161–167 (2002)
17. C. Tu et al., Polym Advan Technol **14**(8), 565–573 (2003)
18. M.H. Ho, P. Kuo, H. Hsieh, T. Hsien, L. Hou, J. Lai, D. Wang, Biomaterials **25**(1), 129–138 (2004)
19. Y.Q. Goh, C.P. Ooi, J Mater Sci Mater Med **19**(6), 2445–2452 (2008)
20. A.G. Mikos et al., Polymer **35**(5), 1068–1077 (1994)
21. P.X. Ma, R. Zhang, J Biomed Mater Res **56**(4), 469–477 (2001)
22. Y. Wan et al., Polym Advan Technol **19**(2), 114–123 (2008)
23. P.v.d. Witte et al., J Polym Sci Part B Polym Phys **34**(15), 2553–2568 (1996)
24. Y. Hu et al., J Biomed Mater Res **59**(3), 563–572 (2002)
25. S. Li et al., Polymer Int **53**(12), 2079–2085 (2004)
26. L. Liu et al., J Biomed Mater Res **82A**(3), 618–629 (2007)
27. N. Rotter et al., J Tissue Eng Regenerative Med **1**(6), 411–416 (2007)